

Lithospheric layering in the North American craton

Huaiyu Yuan¹ & Barbara Romanowicz¹

How cratons—extremely stable continental areas of the Earth’s crust—formed and remained largely unchanged for more than 2,500 million years is much debated. Recent studies of seismic-wave receiver function data have detected a structural boundary under continental cratons at depths too shallow to be consistent with the lithosphere–asthenosphere boundary, as inferred from seismic tomography and other geophysical studies. Here we show that changes in the direction of azimuthal anisotropy with depth reveal the presence of two distinct lithospheric layers throughout the stable part of the North American continent. The top layer is thick (~150 km) under the Archaean core and tapers out on the surrounding Palaeozoic borders. Its thickness variations follow those of a highly depleted layer inferred from thermo-barometric analysis of xenoliths. The lithosphere–asthenosphere boundary is relatively flat (ranging from 180 to 240 km in depth), in agreement with the presence of a thermal conductive root that subsequently formed around the depleted chemical layer. Our findings tie together seismological, geochemical and geodynamical studies of the cratonic lithosphere in North America. They also suggest that the horizon detected in receiver function studies probably corresponds to the sharp mid-lithospheric boundary rather than to the more gradual lithosphere–asthenosphere boundary.

Cratons are continental regions where the Earth’s crust has remained largely undeformed since Archaean times¹. How they were formed and how they survived destruction over timescales of billions of years remains a subject of vigorous debate. Interestingly, the cratonic lithosphere (the crust and the uppermost mantle) presents several distinctive and intriguing geological and geophysical features. Diamonds are found only in cratons or at their borders², seismic velocities remain significantly higher than average down to at least 200 km depth³, and heat flow is low⁴, indicating that the cratonic lithosphere must be thick and cold. Yet there is no observed positive geoid anomaly above cratons⁵, whereas geochemical evidence from mantle xenoliths indicates lithosphere depletion through melt extraction⁶. This has led to the concept of the ‘tectosphere’⁷: that the thick, chemically distinct cratonic lithosphere floats high above the oceans and resists destruction by subduction, owing to its particularly low density and high viscosity, which result in part from dehydration.

It remains a challenge for geodynamicists to explain why thick cratonic keels have resisted progressive entrainment into the mantle by convection⁸. The chemically depleted core may be underlain and surrounded by a thermal, conductive boundary layer^{8–10} that acts as a buffer zone and shields the lithosphere from excessive deformation¹¹.

Determining the thickness of the lithosphere is itself a challenge. Thermally, the intersection of the conductive geotherm with the mantle adiabat defines the base of the lithosphere^{8,12}. However, the thickness of cratonic roots remains poorly defined by seismic tomography. Although thicknesses in excess of 300 km have been suggested, recent estimates, taking into account the effects of anisotropy on seismic velocities, indicate values no larger than 200–250 km (ref. 3), in agreement with results from xenolith and xenocryst thermobarometry^{6,13}, heat flow measurements⁴ and electrical conductivity data¹⁴. Yet receiver function studies, which are more sensitive to fine-scale structure, have largely failed to detect the lithosphere–asthenosphere boundary (LAB) at these depths, indicating that it may not be a sharp boundary underneath cratons. On the other hand, strong compressional-to-shear wave

(P–S) and shear-to-compressional wave (S–P) conversions have been found recently at shallower depths (100–140 km) under stable continental regions^{15–17}, leading some authors to infer that the cratonic lithosphere may be considerably thinner than expected^{15,17}, contradicting tomographic and other geophysical or geochemical inferences. The simplest way to reconcile these results is to consider that the receiver function studies detect an intra-continental discontinuity rather than the LAB¹⁸. Such a discontinuity is consistently found in the analysis of long-range seismic profiles¹⁹ and has been attributed to the presence of a zone of partial melt and/or dehydration around depths of 100 km. Evidence for continental lithospheric layering is well documented from a variety of local and regional studies^{20,21} (see also Supplementary section 1).

Finally, there are two classes of competing hypotheses on the formation of cratonic lithospheric roots¹². The first one invokes underplating by one or more hot plumes and the other invokes accretion by shallow subduction in either a continental or arc setting. The cratonic cores were probably formed under the very different tectonic regime of a hotter Archaean mantle, which would have evolved to present-day plate tectonics sometime in the late Archaean era^{2,6,22}, as a consequence of secular cooling.

Two-layered lithosphere in the North American craton

The North American continent is particularly well suited to the study of the question of lithospheric structure and thickness as a function of age of the overlying crust, because of the presence of a well defined Archaean core surrounded by progressively younger Proterozoic and Palaeozoic provinces^{1,23} (Fig. 1a). Here we present the results of a study of azimuthal anisotropy in the upper mantle beneath North America and illustrate how the change with depth of the orientation of the fast axis of anisotropy provides a powerful tool for the detection of layering in the upper mantle. Anisotropy in the upper mantle is most probably caused by lattice preferred orientation²⁴ and holds clues to dynamical processes responsible for past and present deformation.

¹Berkeley Seismological Laboratory, 209 McCone Hall, Berkeley, California 94720, USA.

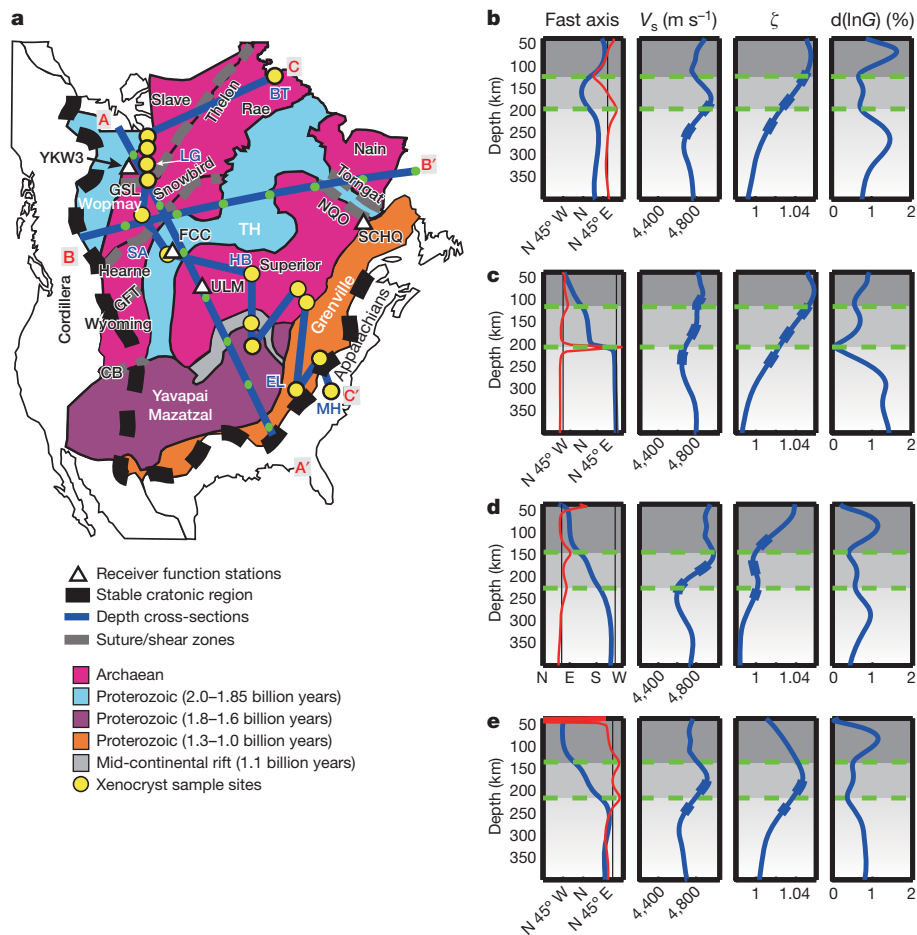


Figure 1 | Precambrian basement age in the North American continent and seismic depth profiles at selected locations. **a**, Precambrian basement age (after ref. 23). The white triangles are the seismic stations used in **b**, and the blue lines are the locations of profiles AA', BB' and CC', discussed in the text. Petrologic sample locations are from ref. 13. The thick dashed black line shows the approximate boundary of the stable parts of the continent, bounded by the Laramide deformation/Rocky Mountain front from the west, and the Ouachita and Appalachian fronts from the south and east¹. The thick dashed grey lines indicate crustal shear zones¹. GSL, the Great Slave Lake shear zone; GFT, the Great Falls tectonic zone; TH, the Trans-Hudson orogen; CB, the Cheyenne belt; NQO and Torngat, shear zones related to the New Quebec orogen and the Torngat orogen, respectively. Blue two-letter labels are Xenocryst sample site names. **b–e**, Seismic depth profiles at stations YKW3 (**b**), ULM (**c**), FFC (**d**) and SCHQ (**e**). Panels show, from left to right, the direction of the fast axis of azimuthal anisotropy, isotropic shear-wave velocity (V_s), radial anisotropy (ζ) and azimuthal anisotropy magnitude (G), respectively. The green dashed lines indicate local maxima in the fast-axis direction gradient as a function of depth, and also delimit three anisotropic layers. The gradient itself is shown as a red line in the fast-axis panels, and the vertical thin black lines denote the North American APM direction²⁶ at the station. (In **c** and **d**, there are two black lines, which show the same APM directions owing to 180° periodicity.) Regions of negative gradients in V_s and ζ are highlighted as thick blue rectangles. Changes in anisotropy direction at depths shallower than 50 km (**d**, **e**) are probably artefacts at the edge of our inversion domain.

This study further refines the methodology developed by Marone and Romanowicz²⁵, and is based upon the joint inversion of long-period seismic waveforms and SKS wave splitting data, using here a much larger data set, providing unprecedented lateral and depth resolution throughout the continent (Supplementary Figs 1 and 2). As shown in ref. 25, models obtained from surface waveforms with or without constraints from SKS splitting measurements reveal the same variations with depth in the orientation of the fast axis of azimuthal anisotropy, but the strength of anisotropy recovered at depths greater than 200 km is larger with the SKS constraints, without degrading the fit to surface waves (see Methods and Supplementary Figs 3, 4 and 5).

In ref. 25, we found that the fast axis of anisotropy systematically changes direction towards the direction of absolute plate motion (APM, as defined in the hotspot reference frame²⁶) at a depth corresponding to the LAB, throughout the North American continent. Here we confirm and refine these results, and we also find that, under the craton, the fast axis of anisotropy changes direction significantly with depth in the upper mantle, not only at around 200 km depth, but also at a shallower depth between 50 and 160 km, depending on

location (Figs 1b–e, 2). This defines two boundaries, each of which is well localized in depth (within about 15 km) and is accompanied by a minimum in the amplitude of azimuthal anisotropy. We note that around the depth of the deeper boundary, the depth profile of isotropic S-wave velocity (V_s) shows a pronounced negative gradient, but, in contrast to azimuthal anisotropy, it does not allow us to locate the transition to better than 50–100 km in depth. Likewise, the radial anisotropy profiles show a gradual decrease with depth, but no localized transition is resolved. We thus define the LAB as the laterally varying horizon marked by the change of fast axis with depth towards the APM (Figs 1b–e, 2, 3a). We note that, east and southeast of the craton, the lithosphere remains thick well into provinces of Proterozoic age. West of the Rocky Mountain Front, on the other hand, it becomes rapidly much thinner (Fig. 3a). We next focus on the Proterozoic and Archaean parts of the continent, and defer further discussion of the tectonically active western part of North America to a separate publication²⁷.

Interestingly, the shallower horizon detected within the craton is often accompanied by a local minimum in the isotropic shear velocity (Fig. 1b–e); this minimum generally falls within the depth range in

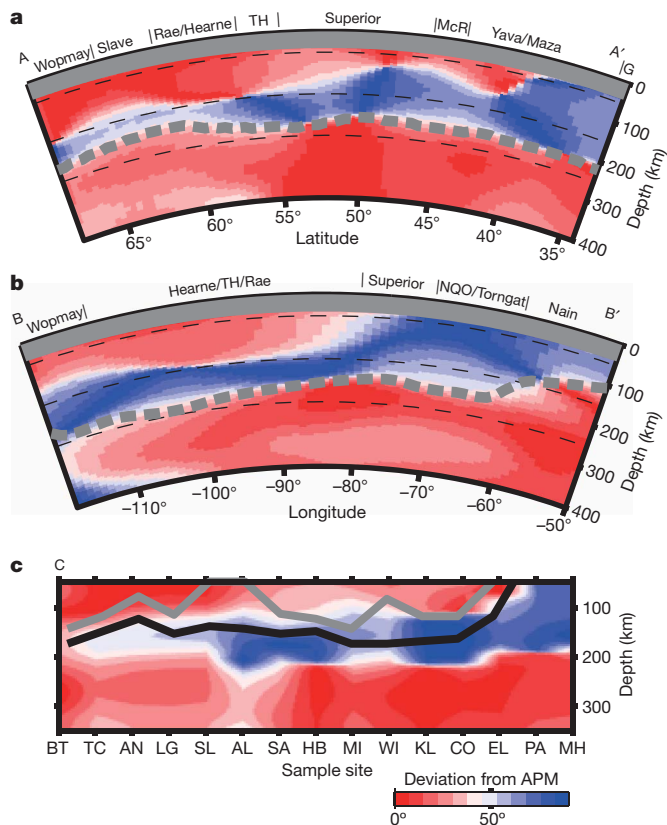


Figure 2 | Upper-mantle layering defined by changes in the direction of the fast axis of azimuthal anisotropy. Depth cross-sections across the three profiles—AA' (a), BB' (b) and CC' (c)—shown in Fig. 1a. The direction of the fast axis is colour-coded as a deviation from the North American APM (see scale)²⁶. The thick dashed line is our inferred LAB. **a**, Yava/Mazat/G, the Proterozoic Yavapai, Mazatzal and Grenville provinces; MCR, the mid-continental rift. **b**, The profile is truncated to the west at the Rocky Mountain front, where the lithospheric character changes abruptly. NQO, Proterozoic New Quebec orogen. **c**, This profile follows the sites where xenocryst samples have been obtained¹³. Sample sites are labelled (two-letter abbreviations) at the bottom of the plot as in Fig. 1. The boundary corresponding to Mg#93 (ref. 13) is indicated by a grey line, and the black line corresponds to Mg#92.

which a negative velocity jump is detected in receiver function studies, and is also consistent with the results of detailed local studies at the locations where these are available (Supplementary Section 1). The depth of this boundary is well resolved by our combined waveform and SKS splitting analysis (Supplementary Figs 6, 7, 8 and 9). This intermediate boundary and the LAB together define three distinct anisotropic layers of variable thickness across the North American craton. The top two layers (herein denoted layers 1 and 2) are contained within the lithosphere, while the deepest layer (layer 3), where the direction of fast axis is consistently sub-parallel to the APM (Supplementary Fig. 11), corresponds to the sub-cratonic asthenosphere.

Continental-scale depth cross-sections (Fig. 2) show that layer 1 is generally thicker in the oldest part of the craton and progressively thins towards younger provinces, tapering out under the Palaeozoic provinces of eastern North America. On the other hand, the lithospheric thickness is relatively constant throughout the Archaean and Proterozoic domains. Studies of xenoliths and xenocrysts in the North American craton have inferred the presence of two chemically distinct domains under the Archaean crust¹³. The top layer is highly depleted, as defined by the corresponding magnesium number ($Mg\# = \text{atomic Mg}/(\text{Mg} + \text{Fe})$; the higher the $Mg\#$, the more depleted the rock), and its thickness varies with the age of the overlying crust. The variations of our layer 1 thickness are in excellent agreement with those of the highly depleted layer as determined geochemically, and roughly coincide with the $Mg\#93$ horizon (Fig. 2c). We thus infer that layer 1 may correspond to the ancient highly depleted Archaean lithosphere, which we are able to resolve and map out across the North American continent, using seismic anisotropy tomography.

Lateral variations in layer 1 and relation to geology

Lateral variations in the fast axis direction are well resolved in our model (Supplementary Figs 8–10). Close inspection of the fast axis direction in layer 1 reveals remarkable consistency with the surface geological trends. For instance, the generally northeast-to-east fast axis direction correlates well with the series of northeast- and east-trending Proterozoic sutures that welded some of the pre-existing Archaean cratons together^{1,28} (Fig. 3b, Supplementary Fig. 11). Northeast of the Superior craton, the northwest-to-southeast fast-axis direction is in good agreement with the northwest-trending New Quebec and Torngat orogens. The change of fast-axis direction from east–west in the western and central Superior to nearly north–northwest

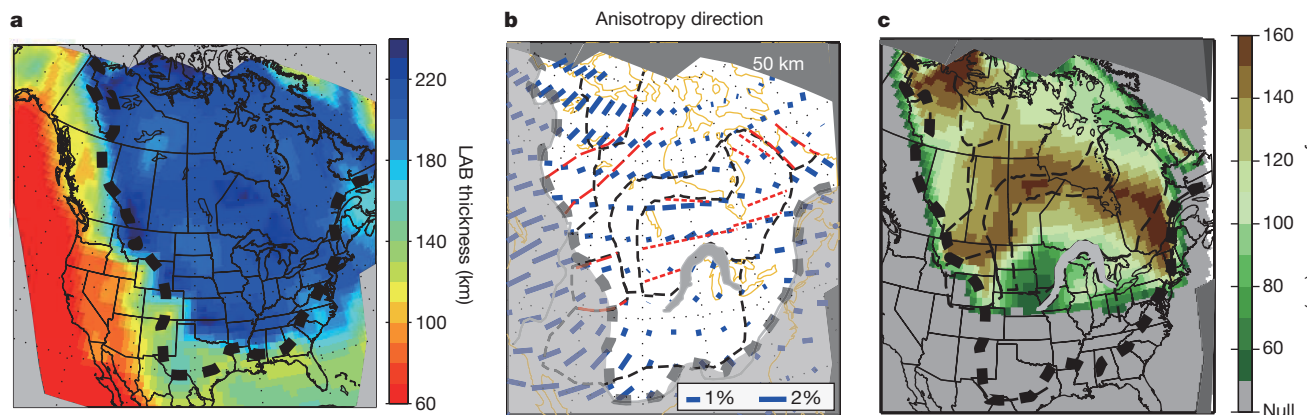


Figure 3 | Thickness and anisotropy of layer 1 and LAB thickness across the North American continent. The thick broken line indicates the borders of the stable part of the continent as in Fig. 1. **a**, Lithospheric (LAB) thickness, determined from changes in the fast axis direction towards the APM²⁶ beneath the Archaean and Proterozoic parts of the continent. The Rocky Mountain front represents a sharp transition to a distinct anisotropic regime, described elsewhere²⁷. **b**, Fast-axis direction and strength of anisotropy at a depth of 50 km in layer 1 (blue bars) and correspondence with main geological sutures. Black dashed lines are the major crustal

province boundaries (from Fig. 1). Suture zones (thick red dashed lines) are inferred from figure 1 of ref. 1: the Great Slave Lake shear zone/Thelon magnetic zone (between Slave and Rae), the Snowbird shear zone (Rae and Hearne), the Great Falls tectonic zone (Hearne/Medicine Hat and Wyoming), and the Cheyenne belt (Wyoming and Proterozoic Yavapai). Thinner red dashed lines (from figure 1b of ref. 29) show approximate subprovince boundaries in the Superior craton. Light grey shading indicates regions outside stable North America; **c**, Map of layer 1 thickness. Light grey shading indicates regions where no layer 1 has been detected.

in the northeastern Superior craton also follows the trends of the geological sutures of the Superior province²⁹. Fossil subductions, revealed as strong mantle reflectors and high-velocity bodies from active and passive seismic studies^{30–32} are found beneath most of these suture zones and generally indicate a subduction direction normal to the suture trends. We note that the fast-axis directions in lithospheric layer 1 and in the asthenosphere (layer 3) are comparable, similar both to surface geological trends and to the APM (Fig. 1b–e, Supplementary Fig. 5). This suggests a resolution to the long-running controversy surrounding the interpretation of SKS splitting measurements in continents in terms of frozen anisotropy³³ versus anisotropy aligned with the present-day flow³⁴: azimuthal anisotropy in layer 1 reflects ancient tectonic events dating back to the late Archaean era, whereas sublithospheric anisotropy reflects present-day tectonics. They both contribute to SKS splitting.

The thickness of layer 1 varies from about 50 km south of the 1.1-billion-year-old mid-continental rift to over 150 km beneath the 1.8-billion-year-old Trans-Hudson orogen and the 1.9-billion-year-old Wopmay orogen¹ (Fig. 3c). We note that the thickest part is not in the region of oldest Archaean crust, but corresponds to the Trans-Hudson orogen, which has an arcuate shape, and may have been formed as part of the continental collision between the Superior craton to the southeast and the Hearne and Rae cratons to the northwest¹. Indeed, the collisional processes of the Proterozoic era have been linked to those presently active in the India/Asia collision zone along the Himalayas³⁵, where the lithosphere is also thickened. Thicker parts of layer 1 are also found in the northwestern corner of our region, affected by the 1.9-billion-year-old Wopmay orogeny¹. The thickening of layer 1 may thus reflect the results of continental collision in the late Archaean era. Layer 1 thins out and disappears on the eastern borderlands of the continent, which have been subjected to Palaeozoic orogenies, and also west of the Rocky Mountain Front, which is subject to even more recent and currently active tectonics. Within the Proterozoic regions, layer 1 is thinnest near the 1.1-billion-year-old mid-continental rift¹, suggesting that the original Archaean lithosphere may have been perturbed subsequently by rifting. In the south, no layer 1 is found in part of the Proterozoic Yavapai/Mazatzal province. On the eastern border of the craton, layer 1 is present in regions where the Proterozoic crust is underlain by Archaean upper mantle³⁶, suggesting that the Archaean lithosphere is probably more laterally extensive at depth than near the surface, and, in places, may be wedged into the more juvenile (Proterozoic province) blocks³⁷. To infer more completely the patterns of anisotropy, and in particular the dip of the axis of symmetry, azimuthal anisotropy needs to be combined with other information, including radial anisotropy³⁸. Under the North

American craton, the velocity of horizontally polarized shear waves, V_{SH} , exceeds that of vertically polarized shear waves, V_{SV} , in general, indicating dominant horizontal shear³⁹. However, significant radial anisotropy anomalies, with $V_{SH} < V_{SV}$, coincide with the location of some of the suture zones (such as the Rae/Hearne and Hearne/Trans-Hudson zones; see Supplementary Fig. 12b, e), suggesting the local presence of anisotropy with dipping axis possibly related to fossil accretion processes⁴⁰. Resolving the dip of the axis involves making strong assumptions on the mineralogy, which is beyond the scope of this paper.

The nature of layer 2

Comparison with the geochemistry studies (Fig. 2c) suggests that layer 2 may represent a younger, less depleted, thermal boundary layer, possibly accreted at a later stage through processes influenced by the presence of a stagnant, chemically distinct lid (layer 1). This scenario is supported by the excellent agreement between the lateral variations in the depth of the LAB inferred from our azimuthal anisotropy study and the variations predicted from the thickness of layer 1 (Fig. 4), when applying the geodynamically inferred relationship between the thicknesses of the chemical and thermal lithospheres^{10,12}. Except for a few locations at the margins of the craton where layer 1 thins out, the overall misfit between the observed and predicted LAB is ± 15 km. While the thickness of layer 1 varies significantly across the stable part of the continent, the lithosphere as defined by the bottom of layer 2 is remarkably flat (depths between 180 and 240 km), including in the Proterozoic provinces where layer 1 has thinned out (Figs 3a, 4a), and as predicted by geodynamical modelling¹⁰. The flat LAB at the bottom of the thermal conductive layer is also in good agreement with local seismic, petrologic and magnetotelluric studies (Supplementary Section 2) and indicates the lack of strong lateral variations in temperature at greater depths below the stable continent, in agreement with the absence of significant topography on the 400-km and 660-km discontinuities⁴¹. When combining azimuthal anisotropy and radial anisotropy results, shorter wavelength variations within layer 2 are observed, which probably hold additional clues on the formation of this layer (Supplementary Fig. 12).

Implications for the formation of continental lithosphere

Here, by using an approach based on seismic azimuthal anisotropy, we have documented the craton-wide presence of a mid-lithospheric boundary, separating a highly depleted chemical layer of laterally varying thickness, from a less depleted deeper layer bounded below by a relatively flat LAB (Fig. 5). Alignment of the fast anisotropy axis

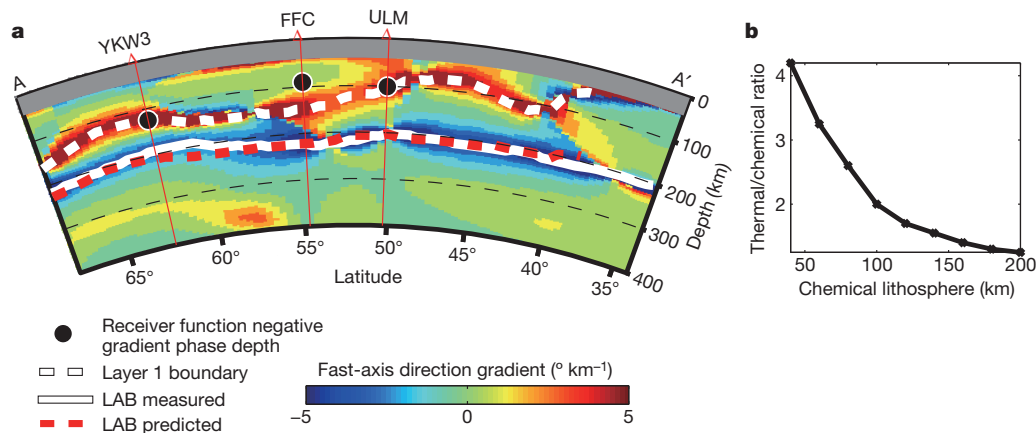


Figure 4 | Relative thickness of layers 1 and 2 along the depth cross-section AA' shown in Figs 1a and 2a. a, Gradient of the fast-axis direction as a function of depth along the profile. Gradient extremes mark the boundaries between layers 1 and 2 (white dashed line) and the LAB (continuous white line). The red dashed line is the prediction of LAB depth from the

geodynamic calculation¹⁰, according to the relation between thickness of chemical (layer 1) and thermal (layer 1 + layer 2) lithosphere (b), and using as input our layer 1 thickness. This is in good agreement with the seismically inferred LAB north of 38° latitude. The black dots indicate depth of boundary detected by receiver function studies^{15–17}.

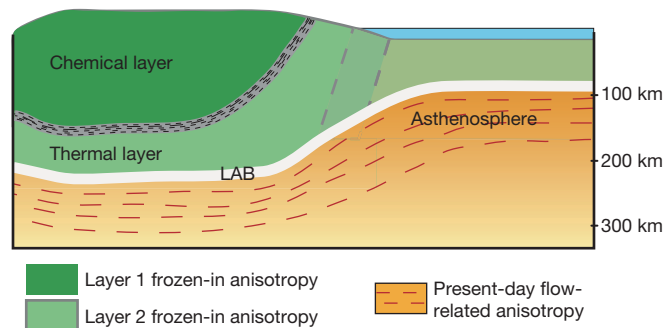


Figure 5 | Cartoon illustrating the inferred stratification of the lithosphere. Beneath the craton, three layers of anisotropy are present: two in the lithosphere (layers 1 and 2), and one in the asthenosphere. Layer 1 corresponds to the chemically distinct, depleted Archaean lithosphere, and layer 2 is the thermal root, separated from the asthenosphere by the LAB, which is at relatively constant depth beneath the stable part of the continent, but rapidly shallows between the tectonic part of the continent (in the western USA) and in the oceans. The boundary between layers 1 and 2 is seismically sharp but its fine-scale structure is likely to be complex. The depth extent of the zone of present-day flow-related anisotropy is not tightly constrained by our study. This figure was modified from ref. 3.

in layer 1 with the old geological sutures indicates that tectonic processes active in the late Archaean era, involving continent–continent collision, may have welded together old Archaean blocks. These blocks may themselves have been formed in a very different tectonic regime²². On the other hand, the fast-axis direction in layer 2 is consistently northerly (Fig. 2 and Supplementary Fig. 11b), in agreement with local studies^{21,42,43}, reminiscent of the trench parallel direction observed in present-day subduction zones⁴⁴. This suggests that the thermal boundary layer might have been formed in a tectonic context involving predominant east–west compression, or, alternatively, that it was formed diffusively while responding to the northerly APM prevalent during the Mesozoic opening of the Atlantic Ocean following the Appalachian orogeny²¹.

A plume hypothesis may be valid for the formation of the depleted Archaean lithosphere^{2,12,45}, provided the fast-axis direction recorded in layer 1 merely reflects subsequent processes welding together the older blocks. However, layer 2 anisotropy directions are not compatible with a plume context for its formation, as we would then expect directions of anisotropy that radiate from one or several central points rather than the uniform north-to-south fast-axis directions we observe. The well preserved and spatially consistent azimuthal anisotropy found in the deep lithosphere under the craton, different from present-day APM, should provide important constraints for future geodynamical modelling of the continent's formation and evolution.

Although the anisotropy modelling presented here cannot by itself precisely determine the sharpness of the detected boundaries, it allows us to reconcile recent receiver function and seismic velocity tomography studies. In particular, we suggest that receiver functions and long-range seismic profiles preferentially detect the transition between the ancient Archaean lithosphere (layer 1) and the subsequently accreted thermal boundary layer (layer 2). The details of this transition and its precise nature are beyond the resolution of our study, but are likely to be complex, as indicated by the fine layering documented by long-range seismic profile studies¹⁹, and, as suggested in these studies, may involve stacks of thin low-velocity layers marking traces of partial melting and dehydration⁴⁶, possibly at the top of oceanic lithosphere that had been welded onto the bottom of layer 1. It could also result from kimberlite accumulation⁴⁷ if the strong, chemically distinct, Archaean layer 1 acts as a barrier to their further ascent.

We note that this mid-lithospheric anisotropic boundary zone must be a sharp high-to-low velocity horizon because it produces converted phases seen in receiver function studies, but it is barely

detectable by isotropic velocity tomography, although we have noted the presence of a local minimum in the depth profile of shear velocity in some parts of our model (such as Fig. 1b, c). On the other hand, the LAB under cratons is probably more gradual, because it is hard to detect with receiver functions, which is consistent with a largely thermal, anisotropic boundary that probably does not involve any significant compositional changes or partial melting. It is possible, in particular, that the boundary detected by ref. 48 in the northeastern USA from receiver functions may be the eastern border of the chemically distinct layer 1, rather than the LAB, which is deeper in this region, as determined by this and other tomographic studies. Further characterization of the mid-lithospheric boundary holds the clue to our better understanding of key geochemical and geodynamical processes of Archaean and early Proterozoic times.

The change of fast-axis direction of azimuthal anisotropy with depth is a powerful tool for the detection of lithospheric layering under continents. Our study indicates that the 'tectosphere' is no thicker than 200–240 km and that its chemically depleted part may bottom around 160–170 km. Although the morphology of the North American craton may be exceptionally simple, the application of this tool to other continents should provide further insights into the assembly and evolution of cratons worldwide.

METHODS SUMMARY

We consider three-component long-period time-domain seismograms, observed at broadband seismic stations in the USA and Canada and low-pass-filtered at periods longer than 60 s. We separately weigh wavepackets corresponding to fundamental modes and overtones, and apply weights to equalize density of paths. The data set is considerably larger than that used in ref. 25 owing to the availability of data from USArray, the Canadian National Seismic Network, and temporary deployments (Supplementary Fig. 1a). We also perform more accurate crustal corrections⁴⁹, accounting for nonlinear effects due to strong lateral variations in crustal thickness, both of which allow us finer-scale depth and lateral resolution (Supplementary Figs 6–10). We correct for propagation outside our target area using a new global upper-mantle model developed using full waveform inversion and a new global tomographic approach using the spectral element method (V. Lekic and B.R., manuscript in preparation). The waveform data are first inverted to obtain a reference continental-scale isotropic and radially anisotropic model with lateral resolution of about 250 km (Supplementary Fig. 1b). We then combine the waveforms with a significantly expanded data set of station-averaged SKS splitting measurements (Supplementary Fig. 2), in a joint inversion for three-dimensional variations in azimuthal anisotropy, using the formalism of ref. 50 for the computation of SKS sensitivity kernels. The additional constraints from SKS splitting data allow us to constrain the azimuthal anisotropy amplitude better below 200 km without degrading the fit to surface waveforms, while explaining a significant portion of the variance in SKS splitting observations (Supplementary Fig. 4) owing to the better amplitude recovery from the combined data sets, as illustrated in the comparison of depth profiles (Supplementary Fig. 5) and in the synthetic tests (Supplementary Figs 6, 7, 8 and 9). Further technical details are given in the online Methods.

Full Methods and any associated references are available in the online version of the paper at www.nature.com/nature.

Received 11 December 2009; accepted 25 June 2010.

- Hoffman, P. F. United plates of America. The birth of a craton: early proterozoic assembly and growth of Laurentia. *Annu. Rev. Earth Planet. Sci.* **16**, 543–603 (1988).
- Haggerty, S. E. A diamond trilogy: superplumes, supercontinents, and supernovae. *Science* **285**, 851–860 (1999).
- Gung, Y., Panning, M. & Romanowicz, B. Global anisotropy and the thickness of continents. *Nature* **422**, 707–711 (2003).
- Mareschal, J. C. & Jaupart, C. Variations of surface heat flow and lithospheric thermal structure beneath the North American craton. *Earth Planet. Sci. Lett.* **223**, 65–77 (2004).
- Shapiro, S. S., Hager, B. H. & Jordan, T. H. The continental tectosphere and Earth's long-wavelength gravity field. *Lithos* **48**, 135–152 (1999).
- Carlson, R. W., Pearson, D. G. & James, D. E. Physical, chemical, and chronological characteristics of continental mantle. *Rev. Geophys.* **43**, doi:10.1029/2004rg000156 (2005).
- Jordan, T. H. Composition and development of the continental tectosphere. *Nature* **274**, 544–548 (1978).

8. King, S. D. Archean cratons and mantle dynamics. *Earth Planet. Sci. Lett.* **234**, 1–14 (2005).
9. Sleep, N. H. Survival of Archean cratonal lithosphere. *J. Geophys. Res.* **108**, doi: 10.1029/2001jb000169 (2003).
10. Cooper, C. M., Lenardic, A. & Moresi, L. The thermal structure of stable continental lithosphere within a dynamic mantle. *Earth Planet. Sci. Lett.* **222**, 807–817 (2004).
11. Lenardic, A., Moresi, L. & Mühlhaus, H. The role of mobile belts for the longevity of deep cratonic lithosphere: the crumple zone model. *Geophys. Res. Lett.* **27**, doi: 10.1029/1999gl008410 (2000).
12. Lee, C. T. in *Archean Geodynamics and Environments* (eds Benn, K., Mareschal, J. C. & Condie, K. C.) 89–114 (American Geophysical Union Monograph, 2006).
13. Griffin, W. L. *et al.* Lithosphere mapping beneath the North American plate. *Lithos* **77**, 873–922 (2004).
14. Jones, A. G. *et al.* The electrical structure of the Slave craton. *Lithos* **71**, 505–527 (2003).
15. Rychert, C. A. & Shearer, P. M. A global view of the lithosphere–asthenosphere boundary. *Science* **324**, 495–498 (2009).
16. Abt, D. *et al.* North American lithospheric discontinuity structure imaged by Ps and Sp receiver functions. *J. Geophys. Res.* doi: 10.1029/2009JB006710 (in the press).
17. Yuan, X., Kind, R., Xueqing, L. & Rongjiang, W. The S receiver functions: synthetics and data example. *Geophys. J. Int.* **165**, 555–564 (2006).
18. Romanowicz, B. The thickness of tectonic plates. *Science* **324**, 474–476 (2009).
19. Thybo, H. & Perchuc, E. The seismic 8° discontinuity and partial melting in continental mantle. *Science* **275**, 1626–1629 (1997).
20. Levin, V., Menke, W. & Park, J. Shear wave splitting in the Appalachians and the Urals; a case for multilayered anisotropy. *J. Geophys. Res.* **104**, 17975–17994 (1999).
21. Deschamps, F., Lebedev, S., Meier, T. & Trampert, J. Stratified seismic anisotropy reveals past and present deformation beneath the East-central United States. *Earth Planet. Sci. Lett.* **274**, 489–498 (2008).
22. Griffin, W. L. *et al.* The origin and evolution of Archean lithospheric mantle. *Precamb. Res.* **127**, 19–41 (2003).
23. Canil, D. Canada's craton: a bottom's-up view. *GSA Today* **18**, 4–11 (2008).
24. Babuska, V. & Cara, M. *Seismic Anisotropy in the Earth* Ch. 5 (Kluwer Academic, 1991).
25. Marone, F. & Romanowicz, B. The depth distribution of azimuthal anisotropy in the continental upper mantle. *Nature* **447**, 198–201 (2007).
26. Gripp, A. E. & Gordon, R. G. Young tracks of hotspots and current plate velocities. *Geophys. J. Int.* **150**, 321–361 (2002).
27. Yuan, H. & Romanowicz, B. Depth dependent azimuthal anisotropy in the western US upper mantle. *Earth Planet. Sci. Lett.* (submitted).
28. Whitmeyer, S. J. & Karlstrom, K. E. Tectonic model for the Proterozoic growth of North America. *Geosphere* **3**, 220–259 (2007).
29. Percival, J. A. *et al.* Tectonic evolution of the western Superior Province from NATMAP and Lithoprobe studies. *Can. J. Earth Sci.* **43**, doi: 10.1139/E1106-1062 (2006).
30. van der Velden, A. J. & Cook, F. A. Relict subduction zones in Canada. *J. Geophys. Res.* **110**, doi: 10.1029/2004jb003333 (2005).
31. Bostock, M. G. Mantle stratigraphy and evolution of the Slave Province. *J. Geophys. Res.* **103**, 21183–21200 (1998).
32. Yuan, H. & Dueker, K. in *The Rocky Mountain Region—An Evolving Lithosphere: Tectonics, Geochemistry, and Geophysics* (eds Randy, G. & Karlstrom, K. E.) Geophysical monograph **154**, 329–345 (American Geophysical Union, 2005).
33. Silver, P. G. & Chan, W. W. Shear wave splitting and subcontinental mantle deformation. *J. Geophys. Res.* **96**, 16429–16454 (1991).
34. Vinnik, L. P., Makeyeva, L. I., Milev, A. & Usenko, A. Y. Global patterns of azimuthal anisotropy and deformations in the continental mantle. *Geophys. J. Int.* **111**, 433–447 (1992).
35. St-Onge, M. R., Wodicka, N. & Ijewliw, O. Polymetamorphic evolution of the Trans-Hudson orogen, Baffin Island, Canada: integration of petrological, structural and geochronological data. *J. Petrol.* **48**, 271–302 (2007).
36. Culotta, R. C., Pratt, T. & Oliver, J. A tale of two sutures: COCORP's deep seismic surveys of the Grenville province in the eastern U.S. midcontinent. *Geology* **18**, 646–649 (1990).
37. Snyder, D. B. Lithospheric growth at margins of cratons. *Tectonophysics* **355**, 7–22 (2002).
38. Montagner, J.-P. & Nataf, H.-C. Vectorial tomography. I. Theory. *Geophys. J. Int.* **94**, 295–307 (1988).
39. Marone, F., Gung, Y. & Romanowicz, B. Three-dimensional radial anisotropic structure of the North American upper mantle from inversion of surface waveform data. *Geophys. J. Int.* **171**, 206–222 (2007).
40. Plomerová, J. & Babuska, V. Long memory of mantle lithosphere fabric—European LAB constrained from seismic anisotropy. *Lithos* doi: 10.1016/j.lithos.2010.1001.1008 (in the press).
41. Li, A., Fischer, K. M., Wyssession, M. E. & Clarke, T. J. Mantle discontinuities and temperature under the North American continental keel. *Nature* **395**, 160–163 (1998).
42. Darbyshire, F. A. & Lebedev, S. Rayleigh wave phase-velocity heterogeneity and multilayered azimuthal anisotropy of the Superior Craton, Ontario. *Geophys. J. Int.* **176**, 215–234 (2009).
43. Li, A., Forsyth, D. W. & Fischer, K. M. Shear velocity structure and azimuthal anisotropy beneath eastern North America from Rayleigh wave inversion. *J. Geophys. Res.* **108**, doi: 10.1029/2002JB002259 (2003).
44. Long, M. D. & Silver, P. G. The subduction zone flow field from seismic anisotropy: a global view. *Science* **319**, 315–318 (2008).
45. Arndt, N. T., Coltice, N., Helmstaedt, H. & Gregoire, M. Origin of Archean subcontinental lithospheric mantle: some petrological constraints. *Lithos* **109**, 61–71 (2009).
46. Mierdel, K., Keppler, H., Smyth, J. R. & Langenhorst, F. Water solubility in aluminous orthopyroxene and the origin of Earth's asthenosphere. *Science* **315**, 364–368 (2007).
47. Sleep, N. H. Stagnant lid convection and carbonate metasomatism of the deep continental lithosphere. *Geochem. Geophys. Geosyst.* **10**, doi: 10.1029/2009gc002702 (2009).
48. Rychert, C. A., Fischer, K. M. & Rondenay, S. A sharp lithosphere–asthenosphere boundary imaged beneath eastern North America. *Nature* **436**, 542–545 (2005).
49. Lekic, V. & Romanowicz, B. A simple method for improving crustal corrections in waveform tomography. *Geophys. J. Int.* **182**, 265–278 (2010).
50. Montagner, J.-P., Griot-Pommeroy, D.-A. & Lave, J. How to relate body wave and surface wave anisotropy? *J. Geophys. Res.* **105**, 19015–19027 (2000).

Supplementary Information is linked to the online version of the paper at www.nature.com/nature.

Acknowledgements We thank the IRIS Data Management Center, the Geological Survey of Canada and the Northern California Earthquake Data Center for providing the waveform data used in this study. Discussion with K. Fischer helped improve the manuscript. We thank K. Liu, R. Allen, M. Fouch, A. Frederiksen and A. Courtier for providing their SKS compilations, and W. Griffin and S. O'Reilly for their North American olivine composition measurements. This study was supported by a grant from the National Science Foundation/EarthScope programme. This is the Berkeley Seismological Laboratory contribution number 10-08.

Author Contributions B.R. developed the concept and methodology of the study. H.Y. assembled the data set, and performed the inversions and the supporting resolution tests. Both authors extensively discussed the results and jointly developed implications. Both authors contributed to writing the paper.

Author Information Reprints and permissions information is available at www.nature.com/reprints. The authors declare no competing financial interests. Readers are welcome to comment on the online version of this article at www.nature.com/nature. Correspondence and requests for materials should be addressed to B.R. (barbara.romanowicz@gmail.com).

METHODS

This study follows the methodology described in refs 25 and 39. We apply a full waveform time domain tomographic inversion method in the framework of the nonlinear normal model asymptotic coupling theory (NACT)⁵¹, to obtain three-dimensional elastic and anisotropic continental-scale structure using the fundamental mode and overtones portion of the three-component seismograms, filtered at periods longer than 60 s. NACT takes into account coupling between modes along and across dispersion branches, thus allowing us to represent the body-wave character of overtones by means of two-dimensional finite frequency kernels in the vertical plane containing source and receiver. We parameterize our model in terms of isotropic V_S , radial anisotropy described by the parameter $\xi = (V_{SH}/V_{SV})^2$, and 2ψ azimuthal anisotropy, described by the coefficients G_c and G_s (ref. 52), which refer to terms in $\cos(2\psi)$ and $\sin(2\psi)$, respectively. Station-averaged SKS apparent splitting parameters, delay time δt and fast-axis direction Φ can be expressed in terms of G_c and G_s , assuming weak anisotropy and periods longer than 10 s (ref. 50; also see Methods in ref. 25). We choose to invert only for the isotropic shear-wave velocity V_S and the anisotropic parameters ξ , G_c and G_s , which are best constrained by the observations. We scale density ρ , compressional-wave velocity V_P and the two other radial anisotropy parameters φ and η (as defined for example in ref. 53) to V_S and ξ using empirical scaling relations⁵⁴. We do not consider the other coefficients ($B_{c,ss}$, $H_{c,s}$ and $E_{c,ss}$, as defined in ref. 54) owing to the insufficient sensitivity of our data set to these parameters.

We complemented the three-component teleseismic waveform data collection of ref. 39 with recent data from permanent and temporary broadband stations in North America, to achieve higher spatial resolution and improved azimuthal coverage. We implemented a denser irregular triangular mesh than refs 25 and 39 had, with the minimum grid knot spacing at ~ 200 km and ~ 400 km for isotropic V_S and anisotropy ξ and G_c and G_s , respectively (Supplementary Fig. 1). Vertically, the model is parameterized in terms of cubic splines⁵⁵ with a finer knot spacing (30–70 km) from 24 km to the transition zone and 100–150 km spacing below 670 km. We also perform accurate crustal corrections⁴⁹, accounting for nonlinear effects due to strong lateral variations in crustal thickness, both of which allow us finer-scale depth and lateral resolution (Supplementary Figs 6–10).

We first inverted the waveform data set simultaneously for the three-dimensional isotropic V_S and radial anisotropic ξ structure in North America, after correcting for propagation effects outside our study region using a newly developed three-dimensional global V_S and ξ model⁵⁶. In the second step, the waveform data set, corrected for the three-dimensional V_S and ξ structure obtained in the first step, was

jointly inverted with station-averaged SKS splitting data for three-dimensional variations in 2ψ azimuthal anisotropy, using the formalism of ref. 50. We do not apply any a priori constraints to the starting azimuthal anisotropy model. We used a least-squares approach⁵⁷ to solve the inverse problem at each step. The contribution to the total waveform variance reduction from the three-dimensional V_S and ξ structure (presented in ref. 58) is $\sim 85\%$, and that of the azimuthal anisotropy part of the model is $\sim 15\%$. The total variance reduction in the waveform data set is 60%.

In ref. 25, we showed that inverting the waveform data alone or jointly with SKS splitting data leads to models of azimuthal anisotropy with the same distribution of fast-axis directions and the same fits to the long-period waveforms, but the model based on surface waveforms alone does not predict the SKS splitting directions well, as found by other authors when comparing surface-wave-derived models of azimuthal anisotropy and SKS splitting data over continents⁵⁰ (Supplementary Fig. 3). The addition of SKS splitting data allows us to constrain better the amplitude of azimuthal anisotropy at depths greater than 200 km without degrading the fit to surface waveforms, while at the same time explaining a significant portion of the variance in SKS splitting observations (55% variance reduction compared to 18% when using waveform data alone; see Supplementary Fig. 4 for example). We confirm these results here, but owing to the considerably larger data set, we are able to attain higher resolution and map two layers in the lithosphere throughout the craton. Further technical details and the results of resolution tests are given in the Supplementary Information.

51. Li, X.-D. & Romanowicz, B. Comparison of global waveform inversions with and without considering cross-branch modal coupling. *Geophys. J. Int.* **121**, 695–709 (1995).
52. Montagner, J.-P. & Nataf, H.-C. A simple method for inverting the azimuthal anisotropy of surface waves. *J. Geophys. Res.* **91**, 511–520 (1986).
53. Panning, M. & Romanowicz, B. A three-dimensional radially anisotropic model of shear velocity in the whole mantle. *Geophys. J. Int.* **167**, 361–379 (2006).
54. Montagner, J.-P. & Anderson, D. L. Petrological constraints on seismic anisotropy. *Phys. Earth Planet. Inter.* **54**, 82–105 (1989).
55. Mégnin, C. & Romanowicz, B. The three-dimensional shear velocity structure of the mantle from the inversion of body, surface and higher-mode waveforms. *Geophys. J. Int.* **143**, 709–728 (2000).
56. Lekic, V. *Inferring the Elastic Structure of the Mantle using the Spectral Element Method* PhD thesis, University of California (2009).
57. Tarantola, A. & Valette, B. Generalized nonlinear inverse problems solved using the least squares criterion. *Rev. Geophys. Space Phys.* **20**, 219–232 (1982).
58. Yuan, H., Romanowicz, B., Fisher, K. & Abt, D. 3-D shear wave radially and azimuthally anisotropic velocity model of the North American upper mantle. *Geophys. J. Int.* (submitted).